

FUNDAMENTAL PHYSICAL PROPERTIES OF LiInS_2 AND LiInSe_2 CHALCOPYRITE STRUCTURED SOLIDS[†]

 Jyoti Kumari^a,  Shalini Tomar^a,  Sukhendra^b,  Banwari Lal Choudhary^a,
 Upasana Rani^a,  Ajay Singh Verma^{c,*}

^aDepartment of Physics, Banasthali Vidyapith, Rajasthan, (India) 304022

^bDepartment of Physics, GDC Memorial College, Bahal, Bhiwani, (India) 127028

^cDepartment of Natural and Applied Sciences, Glocal University, Saharanpur (India) 247232

*Corresponding Author: ajay_phy@rediffmail.com

Received April 6, 2021; accepted June 6, 2021

For the couple of chalcopyrite compounds, we have theoretically studied the various properties for example structural, electronic optical and mechanical properties. The band structure curve, the density of states as well as the total energy have been investigated with the help of ATK-DFT by using the pseudo-potential plane wave method. For the LiInS_2 and LiInSe_2 chalcopyrites, we have found that these compounds possess direct band gap; which is 3.85 eV and 2.61 eV for LiInS_2 and LiInSe_2 respectively. It shows that the band gap is decreasing from 'S' to 'Se' as well as the B/G ratio called Pugh's ratio is 2.10 for LiInS_2 and 2.61 for LiInSe_2 so these compounds are ductile in nature also these compounds are found to be mechanically stable. The study of this work display that the couple of these chalcopyrite compounds can be the promising candidate for the substitution of absorbing layer in the photovoltaic devices.

Keywords: Ab-initio calculations; electronic properties; optical properties; elastic constants

PACS: 31.15.A-; 46.70.-P; 62.20.D-; 62.20.de; 65.40.De; 65.40.-b; 65.60.+a; 71.20.-b

The demand of energy is increasing day by day but the generation of energy without polluting environment is a great challenge now days. The main abundant origin of renewable energy is solar energy and the investigators are concentrated on finding a substitute material which can be used to operate the solar energy as electric power. The photoelectric effect is discovered very firstly by Becquerel [1] and Einstein [2] has given detailed explanation about it. After that the first transistor is made by Shockley et al [3] and gave description about the p-n junction then the work is started on semiconductor devices. Practically the first silicon p-n junction solar cells with the efficiency of 4.5% have been invented by Chapin et al [4]. After that the efficiency of the photovoltaic device approached 6% and then reached 10% [5]. The generation of electricity from the rays of sun is safe, it is reliable, eco-friendly and very rich in resources. Generally, in the manufacturing of a solar cell consists many layers likewise layer of antireflection, layer of window, front electrode, layer of buffer, back electrode, absorbing layer, substrate etc. but the most important layer is absorbing layer in the solar cells and all researchers are concentrated to finding the substitute material for the absorbing layer of the solar cell which should be lower in cost, non-toxic, pollution free and having better efficiency [6]. For the purpose of conversion of energy, the perovskites and the chalcogenides are considered as potential materials but the chalcopyrite display some extent of distinctive performance [5]. The silicon based solar cells are very expensive and for the global application of solar cells needs a huge reduction in the cost of photovoltaic cells. In photovoltaic technology, renewable energy resource is the main source having the biggest possibility in the reduction of cost and efficiency gains. If we are comparing the perovskite and the chalcogenides; then we will get that the chalcogenides having the good potential for the photovoltaic applications in some aspects. In the recent scenario [7-9], the ternary chalcopyrite compounds attract the interest of researchers towards themselves. The chalcopyrite based photovoltaic devices have the very excessive tolerance to every radiation also their life time was found 50 times longer than a silicon-based device [10]. The variation in the band gaps of these chalcopyrite compounds from IR region to UV region matches with the solar spectrum and these compounds can be grown up in the form of thin films by which these compounds are potential candidate for the employment in the solar cells [11]. The chalcopyrite compounds have the general composition $\text{A}^{\text{I}}\text{B}^{\text{III}}\text{X}_2^{\text{VI}}$ and these compounds having many applications likewise light emitting diodes [12], optical devices, non-linear optical devices [13], tunable laser system [14]. The chalcopyrite structured solids having tetragonal symmetry space group I42d (N^o 122) [15]. LiInSe_2 chalcopyrite compound is the most promising candidate for the applications in photovoltaic devices [16]. The properties like thermodynamic, mechanical properties, lattice dynamics are investigated theoretically of the chalcopyrite compounds LiInS_2 , LiInSe_2 and LiInTe_2 [17-20] also the piezoelectric and mechanical properties of LiMX_2 compound, (where M = Ga, In and X = S, Se) have reported [21]. Also, by using the CASTEP code the optical, structural and electronic properties of LiInS_2 and LiInTe_2 chalcopyrite material have reported [17]. Now days the efficiency of lithium-based chalcopyrite materials have crossed from 22.8% [22,23].

Here, we have investigated the lattice dynamics, elastic properties, total energy, optical spectrum, electronic properties of the LiInS_2 and LiInSe_2 chalcopyrite compounds. There is lack of information is provided about the optical properties of these compounds so we are working on these crystal compounds to fill this lack of information.

[†] Cite as: J. Kumari, S. Tomar, Sukhendra, B.L. Choudhary, U. Rani, A.S. Verma, East. Eur. J. Phys. 3, 62 (2021), <https://doi.org/10.26565/2312-4334-2021-3-09>

COMPUTATIONAL METHOD

For the group of chalcopyrite compounds, we have theoretically investigated the structural properties, optical properties, mechanical properties, electronic properties, total energy by using the ATK-VNL (Atomistic Tool Kit-Virtual Nano Lab) simulation package [24]. It is a pseudo-potential plane wave method within the framework of (DFT) density functional theory [25-26]. ATK-VNL is a commercially licensed simulation package. For the investigation of above-mentioned properties, we have used the double zeta polarized basis sets for the electron wave function expanding and for the exchange correlation function we have used the GGA-PBE. The structures are permitted to optimize until each atom achieve force convergence criteria 0.05 eV/Å and the maximum stress is 0.05 eV/Å³. Maximum numbers of steps performed are 200 for the process of optimization and during this process maximum step size 0.2 Å which is also fixed. The convergence is achieved by deciding mesh cut-off energy on the ground of convergence principle and for this calculation 75 Hartree has been projected all over calculation as the most favourable after several convergence tests. For the spin polarization, no spin initial state has been selected for the atoms. We used the 24 x 24 x 24 Monk Horst-Pack k-mesh for the brillouin zone sampling to maintain balance between the calculation time and the results accuracy [27]. Further, all the constrain cell in x, y and z directions are removed for the optimization of crystal structure.

RESULTS AND DISCUSSION

Structural properties

The ternary chalcopyrite compounds LiInS₂ and LiInSe₂ are crystallize in the symmetry of body centred tetragonal and the space group is I42d and the space group number is 122. The configuration of atoms in the crystal structure after optimization of LiInS₂ and LiInSe₂ compounds have been illustrated in the Fig. 1 and the optimized lattice constants (a and c in Å) for these configurations in comparison with the experimental data are described in Table 1 and have been concluded that the calculated lattice constants are closer to the experimental values of the lattice constants. Also, the calculated total energy of LiInS₂ compound is -2617.97794 eV and for LiInSe₂ compound is -2756.35359 eV at which these compounds are optimized.

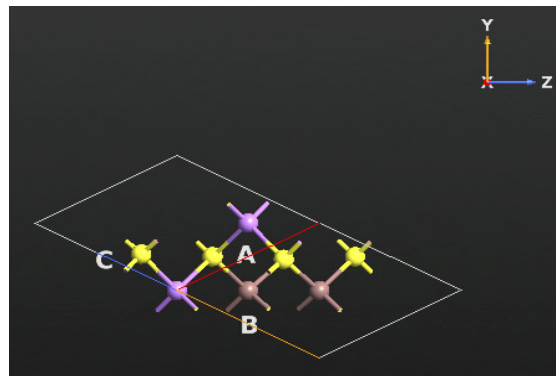


Figure 1. Atomic arrangement in chalcopyrite compounds LiInX₂ (X=S, Se) configurations. Purple color represents A-atom (Li), Brown color represents B-atom (In) and Yellow color represents C-atom (S and Se).

Table 1. Structural Parameters of LiInX₂ (X=S, Se) chalcopyrite compounds.

Compounds	Lattice Constants			
	Calculated		Experimental	
	a (Å)	c (Å)	a (Å)	c (Å)
LiInS ₂	5.523	11.120	5.996 ^{Ref [38],*}	11.078 ^{Ref [38],*}
LiInSe ₂	5.618	11.303	5.807 ^{Ref [38]}	11.810 ^{Ref [38]}

* experimental data.

Electronic properties

The optical properties of a compound are basically depending on the results of the electronic properties of that compound it means if we are getting more accurate band structure then we will be get more accurate optical properties. We have described the band structure of LiInS₂ and LiInSe₂, in this investigation of band structure the GGA-PBE exchange correlation potential have been used to execute the scf calculations using optimized lattice dynamics. The band structure curves between the wave vector 'k' and the energy functional of these compounds, plotted in the first brillouin zone are shown in the Figure 2 (a) and (b). This investigation of electronic band structure reveals that these couple of compounds are direct band gap semiconductors and the directivity of these compounds lies on $\Gamma - \Gamma$, for these compounds the computed energy band gap of LiInS₂ is 3.85 eV and for LiInSe₂ is 2.61 eV respectively.

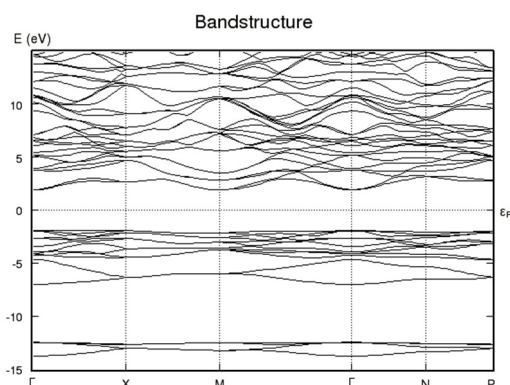


Figure 2 (a): Band structure plots of LiInS₂

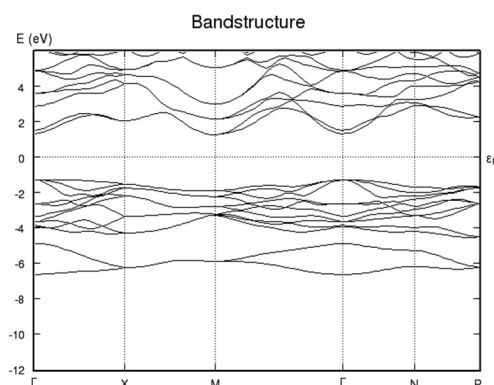


Figure 2 (b): Band structure plots of LiInSe₂

The reduction in the energy band gaps from the replacement of sulphur atom to the selenium atom in LiInX₂ chalcopyrite compound can be accredited to the modification of the conduction bands near the Fermi level, which reflects the important role of S in the band gap opening if the valence band is remains unaffected [28]. The calculated values of band gap are closer to the experimentally extracted energy band gap 3.57 eV for LiInS₂ and 2.83 eV for LiInSe₂ [29]. By doing the study of band structure of a compound, we have find out the band-gap of a compound; which is helpful to deciding the nature of the material likewise it is semiconductor, metallic or non-metallic in nature. We find out these couple of compounds LiInX₂ (X = S and Se) are the direct band-gap semiconductors and values are presented in Table 2.

Table 2. Electronic and Optical Parameters of LiInX₂ (X=S, Se) Chalcopyrite compounds.

Compounds	Band Gap (eV)		Dielectric Constant
	Calculated	Experimental	
LiInS ₂	3.85	3.57 ^{Ref [29]}	2.085
LiInSe ₂	2.61	2.83 ^{Ref [29]}	2.884

For the further understanding of electronic properties, we have been investigated the DoS (Density of States) of these compounds. The computed electronic band have been allocated with the help of the graphs of density of state and shown in the Figure 3 (i) DoS of LiInS₂ and (ii) DoS of LiInSe₂ by using the GGA-PBE exchange correlation potential.

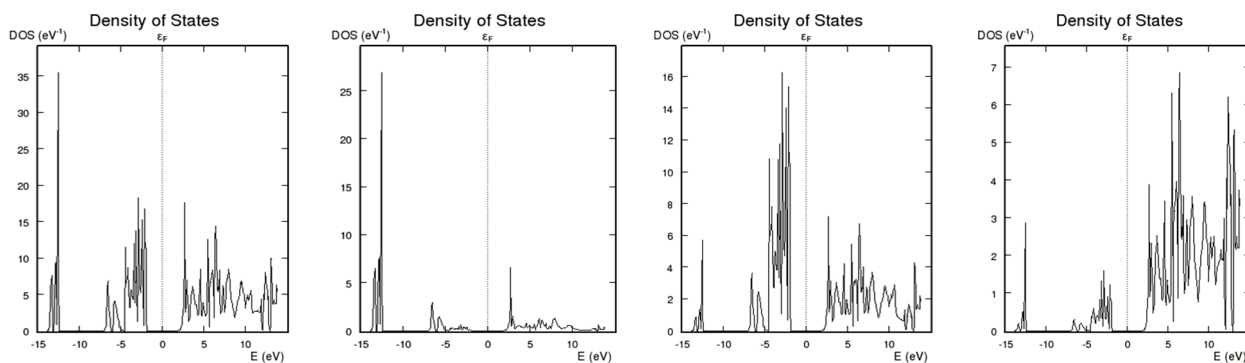


Figure 3 (i). (a) Total DOS of LiInS₂ compound.

Figure 3 (i). (b) Contribution of s-state in LiInS₂ compound.

Figure 3 (i). (c) Contribution of p-state in LiInS₂ compound.

Figure 3 (i). (d) Contribution of d-state in LiInS₂ compound.

We have plotted the total density of state graphs for the analysis of the influence of the different states of atoms for the valence and the conduction band. In the Figure 3 (i) (a) we have plotted the graph of total density of states of LiInS₂ chalcopyrite compound, in which the combined contribution of s, p and d states in the valence and conduction band region. In the Figure 3 (i) (b) we have plotted the density of state graph of the contribution of s-state, we got the major peak of s-state separated by small energy intervals so in this region the contribution of s-state is very high on the other hand, the contribution of s-state in the conduction band is very less as compare it's contribution in valence band. In Figure 3 (i) (c) shows the graph of density of state of the contribution of p-state, we got the major peaks of p-states at a particular energy intervals so the contribution of p-state in the valence band region is more than it's contribution in the conduction

band region, Figure 3 (i). (d). shows the graph of density of state of contribution of d-state, we got the major peaks of d-state at the particular energy intervals so the contribution of d-state is more in the conduction band region as compare it's contribution in the valence band region. Similarly, we have presented for LiInSe_2 in Figure 3 (ii) (a-d).

From the analysis of these graphs of density of states of LiInS_2 chalcopyrite compounds we observed that in the region of valence band there is s-p hybridization is formed and the contribution of d-state is very less as compare to the contribution of s and p states on the other hand in the conduction band there is p-d hybridization is formed and the contribution of s state is less as compare to the contribution of p and d states. We have observed that the calculated band structure and the density of states exhibit identical behaviour.

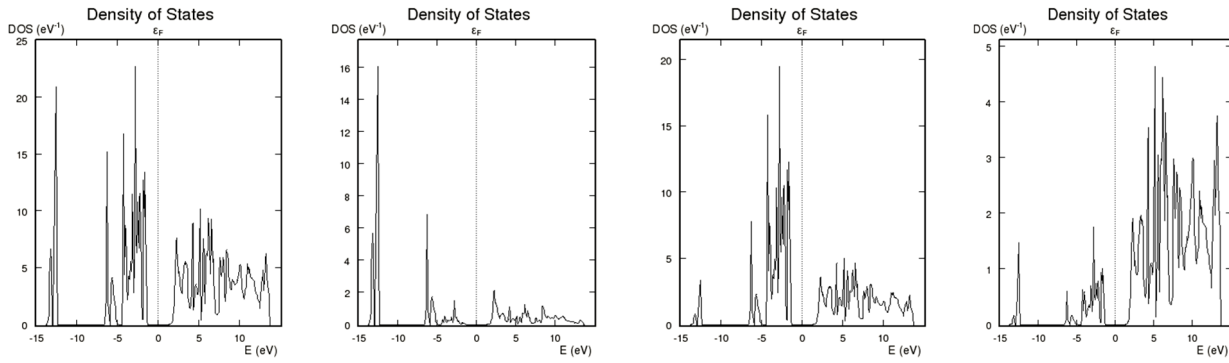


Figure 3 (ii). (a) Total DOS of LiInSe_2 compound.

Figure 3 (ii). (b) Contribution of s-state in LiInSe_2 compound.

Figure 3 (ii). (c) Contribution of p-state in LiInSe_2 compound.

Figure 3 (ii). (d) Contribution of d-state in LiInSe_2 compound.

Elastic Properties

The most fundamental properties of a semiconducting material are the elastic properties. As we all know very well the elastic properties gives the valued data regarding the binding characteristics between the adjacent planes. Usually, the anisotropic coefficients of binding and the stability of structure are described by the elastic constants C_{ij} . These elastic constants provide us the very significant data likewise stability of the crystal structure, mechanical properties, bond indexes and the anisotropy of material. These elastic moduli need the good information regarding the derivative of the energy as a function of the lattice strain [30]. From the elastic constants we can derive the mechanical properties likewise the bulk modulus, shear modulus, young's modulus, and poisson's ratio etc. and these moduli are playing most important role in finding the strength of the materials also these elastic properties defines that how a material undergoes stress deforms and then recovers and returns to its original shape after stress ceases. Moreover, the elastic constants of crystal structure of solids give the relation in between the mechanical and dynamical behaviours of solids also provide the essential data about the nature of the forces applying in the solids.

For a stable tetragonal crystal structure of a solid, mainly there are six independent elastic constants C_{ij} (C_{11} , C_{12} , C_{13} , C_{33} , C_{44} and C_{66}) must fulfil the well-known Born–Huang conditions for the stability of the solid crystals [31]. These elastic constants are related to the bulk modulus B_0 and the five shear constants ($C_{11} + C_{12}$, $C_{11} + C_{12} + 2C_{33} - 4C_{13}$, $1/2C_{33}$, $C_{11} - C_{12}$ and $1/2C_{66}$). Hereafter, a set of five equations required to determine all constants, the first equation contains the bulk modulus B_0 , which is related to the elastic constant by

$$B_0 = \frac{(C_{11} + C_{12})C_{33} - 2C_{13}^2}{C_{11} + C_{12} + 2C_{33} + 4C_{13}^2} \quad (1)$$

In the body centred tetragonal crystal structure of a solid the necessities of the mechanical stability having limitations on the elastic constants which are as follows;

- $C_{11} > 0$, $C_{33} > 0$, $C_{44} > 0$, $C_{66} > 0$,
- $(C_{11} - C_{12}) > 0$, $(C_{11} + C_{33} - 2C_{13}) > 0$,
- $\{2(C_{11} + C_{12}) + C_{33} + 4C_{13}\} > 0$.

The most important elastic properties are Zener anisotropy factor generally we denoted by 'A', Young's modulus denoted by 'E', Poisson's ratio denoted by 'σ' for the applications are computed with help of following relations [32];

$$A = \frac{C_{44}}{C_{11} - C_{12}} \quad (2)$$

The stability of the crystal structure is obtained by the anisotropic factor 'A', the material is isotropic if the value of 'A' is equal to one and the material is anisotropic if the value of 'A' deviate from one. The isotropic materials are those materials whose properties does not depends on the direction called isotropic materials.

$$\sigma = \frac{1}{2} \left[\frac{B-2/3 G}{B+1/3 G} \right] \quad (3)$$

The [3] is the value of Poisson's ratio in the terms of b and G and for most of the materials the value of σ lies in between 0 to 0.5.

$$E = \frac{9GB}{G+3B} \quad (4)$$

The 'E' [4] is young's modulus in the terms of B and G and it is used to determine the stiffness of the materials.

$$G = \frac{G_V + G_R}{2} \quad (5)$$

Here, G is the anisotropic shear modulus,

G_V is the Voigt's shear modulus corresponding to the upper bound values of G,

and G_R is the Reuss's shear modulus corresponding to the lower bound values of G.

- $G_V = 1/30 (4C_{11} + 2C_{33} - 4C_{13} - 2C_{12} + 12C_{44} + 6C_{66})$
- $G_R = 15 [(18B_V / C^2) + [6/ (C_{11} - C_{12})] + (6/C_{44}) + (3/C_{66})]^{-1}$
- $B_V = (1/9) [2(C_{11} + C_{12}) + C_{33} + 4C_{13}]$
- $C^2 = (C_{11} + C_{12}) C_{33} - 2(C_{13})^2$

In the above stated formulas, the subscript refers V to Voigt bound, R refers to Reuss bound [33]. The material is soft or hard it can be decided by the value of bond index if the value of bond index is less than 12 then the material is soft if the value of bond index is more than 12 then the material is hard [34]. The material is brittle or ductile it can be decided by the Pugh's ratio B/G if this ratio is less than 1.75 then the material is brittle and if this ratio is more than 1.75 then the material is ductile. The ratio B/G is a simple relationship related to the brittle or ductile nature of the material [35]. We can determine the mechanical properties of the material by the young's modulus 'E', Bulk modulus 'B', shear modulus 'G', Poisson's ratio ' σ ' by the Voigt-Reuss-Hill averaging method [36]. All the calculated elastic constants are presented in table 3, 4 and 5.

Table. 3. The calculated elastic constants of LiInX₂ (X=S, Se) chalcopyrite compounds.

Compounds	Elastic constants (GPa)					
	C ₁₁	C ₁₂	C ₁₃	C ₃₃	C ₄₄	C ₆₆
LiInS ₂	55.34	55.77	71.75	30.58	29.39	27.26
LiInSe ₂	72.13	72.11	81.82	27.53	27.43	26.81

From the table 3, we conclude that the mechanical stability limitations for the tetragonal crystal structure $C_{11} > 0$, $C_{33} > 0$, $C_{44} > 0$, $C_{66} > 0$, $(C_{11} - C_{12}) > 0$, $(C_{11} + C_{33} - 2C_{13}) > 0$ and $2((C_{11} + C_{12}) + C_{33} + 4C_{13}) > 0$ are satisfied by all these three chalcopyrite compounds LiInX₂ where (X=S, Se). So, by this calculation of elastic constants, we can say that these compounds possess the tetragonal symmetry.

From the Table 4 (a) and 4 (b) we observed that the value of Poisson's ratio lies in between 0 to 0.5 for these chalcopyrite compounds so we can say that the interatomic forces in these compounds are central forces because the one and only Poisson's ratio gives the more information regarding the characteristics of the bonding forces than any other of the elastic constants. For the central forces in the solid crystals the lower and the upper limits of this ratio are given 0.25 to 0.5 respectively. It shows that, the interatomic forces in these compounds are central forces. From Table 5, we have concluded that the anisotropy factor 'A' deviated from one for these chalcopyrite compounds so these compounds are anisotropic in nature also, the value of B/G is more than 1.75 for all compounds so it confirms that these compounds are ductile in nature.

Table 4. (a) and (b) Elastic Parameters of LiInX_2 (X=S, Se) Chalcopyrite compounds

(a) For LiInS_2		Reuss	Voigt	Hill
Bulk modulus:		42.9693	44.1156	43.5425
Shear modulus:		18.8437	22.4971	20.6704
Young's modulus:	X		Y	Z
		31.0883	31.3485	40.589
Poisson's ratio:	XY		XZ	YZ
		0.3772	0.4212	0.4184
	YX		ZX	ZY
		0.3740	0.3226	0.3231
(b) For LiInSe_2		Reuss	Voigt	Hill
Bulk modulus:		55.4550	55.7677	55.6114
Shear modulus:		20.2216	22.2306	21.2261
Young's modulus:	X		Y	Z
		38.2671	38.3226	44.6953
Poisson's ratio:	XY		XZ	YZ
		0.4005	0.3998	0.3972
	YX		ZX	ZY
		0.4000	0.3423	0.3406

Table 5. Calculated anisotropy factor (A) and Pugh's ratio (B/G) of the LiInX_2 (X=S, Se) compounds.

Compounds	A	B / G
LiInS_2	-68.3488	2.1055
LiInSe_2	1371.5	2.6199

From all the above calculations of elastic properties we concluded that these LiInX_2 (X=S, Se) chalcopyrite compounds are mechanically stable compounds.

Optical Properties

Whenever a material is used in optoelectronic device then for knowing the behaviour of that material the optical properties play an important role. The interaction of a material with electromagnetic radiation can be described by the optical properties and this interaction defines its optoelectronic applications [37-39]. We have been studied the optical properties of the couple of chalcopyrite compounds LiInX_2 (X = S and Se). In the present work, we have calculated the optical parameters, likewise the dielectric function, absorption coefficient and electron energy loss as a function of photon energy. The optical parameters of the interested materials have been computed for the rising energy of the incident electromagnetic radiation ranging from 0 to 5 eV, which is shown in Figure 4. From the computation of these parameters, we can say that these compounds are homogeneous as well as isotropic compounds it means for these compounds the values of different optical parameters are constant with changing the direction of incident electromagnetic radiation's electric field vector, but they are variable with its frequency.

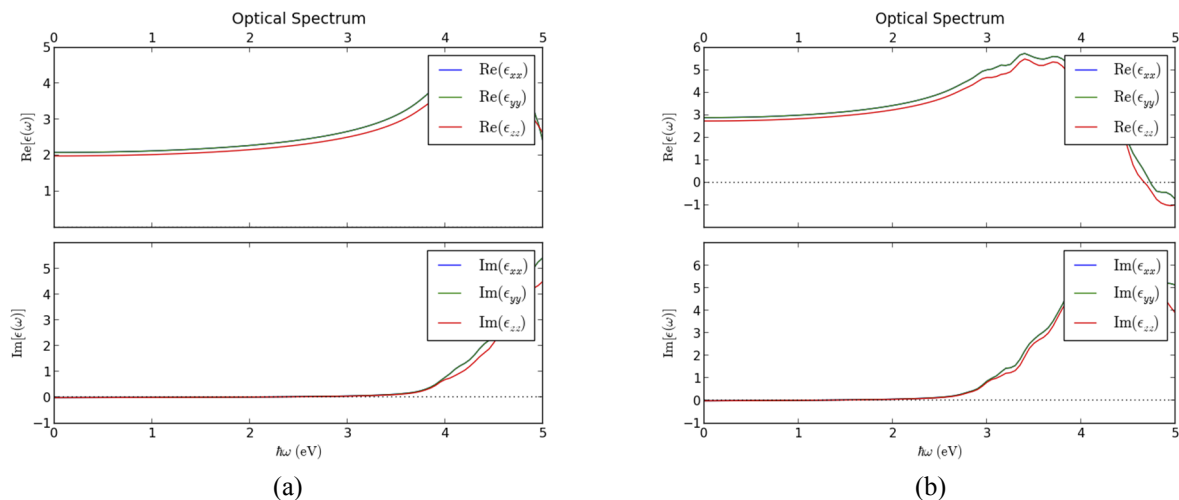
**Figure 4.** Dielectric tensor spectra (a) LiInS_2 and (b) LiInSe_2 compounds for its real part and imaginary part.

Figure 4 shows the real and the imaginary elements of the dielectric tensor spectra $\epsilon(\omega)$ for the energy of incident radiation. The dielectric constant of the compound expresses by the stationary value of its real component also can be defined via a trivial perimeter of the energy. It has been noted that the value of real component of LiInS_2 compound is

2.085 and 2.884 for LiInSe_2 compound. The higher value of real component is responsible for a compound's better response to the incident electromagnetic radiations. Figure 4 displays the variation in real component of the chalcopyrite compounds with the energy of incident radiation. We are clear from the figures of the considered compounds that the value of real component at the particular range of energy (0 eV to 2.98 eV for LiInS_2 and 0 eV to 2.69 eV for LiInSe_2) as the value of energy increases then the value of real component starts raising at a particular range of energy (3.90 eV to 4.78 eV for LiInS_2 and 2.96 eV to 3.97 eV for LiInSe_2) then decreases rapidly and becomes negative (negative is only for the LiInSe_2 compound), later a slightly rising towards zero is observed (only in LiInSe_2 compound). For these two chalcopyrite compounds, the highest value of real component has been observed in UV region i.e., in the UV region of EM spectrum these chalcopyrite compounds give the extreme response. Also, we have observed that the threshold energy of imaginary component varies from 3.92 eV to 4.16 eV for LiInS_2 compound and 2.97 eV to 4.15 eV for LiInSe_2 compound. The value of threshold energy displays the optical band gap of a material and in this study, it is found to be identical to the measured electronic energy band-gap which confirms the good accuracy of proposed results. Moreover, it has been noticed that these compounds, displays a sharp peak of imaginary component. The main peak of imaginary component can be given to the transition of electrons among the valence band maxima and conduction band minima. In this study the optical band gap is found close to the electronic energy band gap so these materials can be the promising material for the photovoltaic applications.

SUMMARY AND CONCLUSIONS

In this research paper, we inspected several physical properties such as structural, electronic, optical and the mechanical properties of LiInX_2 ($X = \text{S}$ and Se) chalcopyrite compounds by using ATK-VNL simulation package. These compounds crystallize in tetrahedral symmetry with the space group $I42d$. They exhibit the direct electronic energy band gap ($\Gamma-\Gamma$) 3.85 eV for LiInS_2 and 2.61 eV for LiInSe_2 , which are having the good agreement with the experimental results. Also, satisfied the optical band gap these materials are good photovoltaic in the UV region of the EM spectrum so these materials act as robust shields for the high energy UV radiations also these can be better photovoltaics in the IR region and the visible region of the EM spectrum. The computed dielectric constant for LiInS_2 is 2.085 and 2.884 is for LiInSe_2 compounds, which is responsible for a compound's better response to the incident electromagnetic radiations. These compounds are mechanically stable compounds and these are ductile in nature because the Pugh's ratio is greater than 1.75 for both of these compounds. Moreover, Poisson's ratio lies in between 0 to 0.5 for these chalcopyrite compounds so we can say that the interatomic forces in these compounds are the central forces. Also, in this computation these compounds are found to be anisotropic because the value of A is < 1 for LiInS_2 and A is > 1 for LiInSe_2 . From the study of this work, we conclude that these materials can be the potential candidate for the photovoltaic applications. The majorities of the parameters explored are reported for the first time to the best of our knowledge and will further stimulate research in the related field.

ORCID IDs

- Jyoti Kumari, <https://orcid.org/0000-0002-1895-158X>; • Shalini Tomar, <https://orcid.org/0000-0001-7385-3061>;
• Sukhendra, <https://orcid.org/0000-0002-2149-5669>; • Banwari Lal Choudhary, <https://orcid.org/0000-0002-0446-8984>;
• Upasana Rani, <https://orcid.org/0000-0003-2550-0442>; • Ajay Singh Verma, <https://orcid.org/0000-0001-8223-7658>

REFERENCES

- [1] E. Becquerel, *Compt. Rend.* **9**, 561 (1839).
- [2] P.C. Deshmukh, and S. Venkataraman, *100 years of Einstein's photoelectric effect*, Bulletin of Indian Physics Teachers Association. (2006).
- [3] S.M. Sze, *Semiconductor devices: physics and technology*, (Wiley John & Sons, 2008).
- [4] D.M. Chapin, C.S. Fuller, and G.L. Pearson, *J. Applied Physics*, **25**, 676-677 (1954), <https://doi.org/10.1063/1.1721711>.
- [5] M. Jing, J. Li, and K. Liu, *IOP Conference Series: Earth and Environmental Science* IOP Publication, **128**, 012087 (2018), <https://doi.org/10.1088/1755-1315/128/1/012087>.
- [6] Q. Lei, Z. Chunmei, and C. Qiang, *Sci. Technol.* **16**, 45 (2014), <https://doi.org/10.1088/1009-0630/16/1/10>
- [7] A.H. Reshak, M.G. Brik, and S. Auluck, *J. Applied Physics*, **116**, 103501 (2014), <https://doi.org/10.1063/1.4894829>.
- [8] J.E. Jaffe, and A. Zunger, *Physical Review B*, **28**, 5822 (1983), <https://doi.org/10.1103/PhysRevB.28.5822>.
- [9] C. Rincon, and C. Bellabarba, *Physical Review B*, **33**, 7160 (1986), <https://doi.org/10.1103/PhysRevB.33.7160>.
- [10] S. Sharma, A.S. Verma, R. Bhandari, and V.K. Jindal, *Computational materials science*, **86**, 108-117 (2014), <https://doi.org/10.1016/j.commatsci.2014.01.021>.
- [11] A.H. Reshak, and M.G. Brik, *J. Alloys and Compounds*, **675**, 355-363 (2016), <https://doi.org/10.1016/j.jallcom.2016.03.104>.
- [12] J.L. Shay, L.M. Schiavone, E. Buehler, and J.H. Wernick, *J. Applied Physics*, **43**, 2805-2810 (1972), <https://doi.org/10.1063/1.1661599>.
- [13] B.F. Levine, *Physical Review B*, **7**, 2600 (1973), <https://doi.org/10.1103/PhysRevB.7.2600>.
- [14] A. Sajid, S. Sajid, G. Murtaza, R. Khenata, A. Manzar, and S.B. Omran, *J. Optoelectronics and Advanced Materials*, **16**, 76-81 (2014), <https://joam.inoe.ro/articles/electronic-structure-and-optical-properties-of-chalcopyrite-cuyz2-yal-ga-in-zs-se-an-ab-initio-study/fulltext>.
- [15] A. Rockett, and R.W. Birkmire, *J. Applied Physics*, **70**, 81-97 (1991), <https://doi.org/10.1063/1.349175>.
- [16] M. Magesh, A. Arunkumar, P. Vijayakumar, G.A. Babu, and P. Ramasamy, *Optics and Laser Technology*, **56**, 177-181 (2014), <https://doi.org/10.1016/j.optlastec.2013.08.003>.

- [17] C.G. Ma, and M.G. Brik, Solid State Communications, **203**, 69-74 (2015), <https://doi.org/10.1016/j.ssc.2014.11.021>.
- [18] A.V. Kosobutsky, and Y.M. Basalae, Solid State Communications, **199**, 17-21 (2014), <https://doi.org/10.1016/j.ssc.2014.08.015>.
- [19] A.V. Kosobutsky, and Y.M. Basalae, J. Physics and Chemistry of Solids, **71**, 854-861 (2010), <https://doi.org/10.1016/j.jpcs.2010.03.033>.
- [20] A.V. Kosobutsky, Y.M. Basalae, and A.S. Poplavnoi, Physica Status Solidi (b), **246**, 364-371 (2009), <https://doi.org/10.1002/pssb.200844283>.
- [21] B. Lagoun, T. Bentria, and B. Bentria, Computational materials science, **68**, 379-383 (2013), <https://doi.org/10.1016/j.commatsci.2012.11.010>.
- [22] L. Isaenko, P. Krinitsin, V. Vedenyapin, A. Yelisseyev, A. Merkulov, J.J. Zondy, and V. Petrov, Crystal Growth and Design, **5**, 1325-1329 (2005), <https://doi.org/10.1021/cg050076c>.
- [23] M.S. Yaseen, G. Murtaza, and R.M.A. Khalil, Current Applied Physics, **18**, 1113-1121 (2018), <https://doi.org/10.1016/j.cap.2018.06.008>.
- [24] Atomistic Toolkit-Virtual Nano lab (ATK-VNL) Quantum wise Simulator, Version. 2014.3, <http://quantumwise.com/>.
- [25] Y.J. Lee, M. Brandbyge, M.J. Puska, J. Taylor, K. Stokbro, and R.M. Nieminen, Physical Review B, **69**, 125409 (2004), <https://doi.org/10.1103/PhysRevB.69.125409>.
- [26] K. Schwarz, J. Solid-State Chemistry, **176**, 319-328 (2003), [https://doi.org/10.1016/S0022-4596\(03\)00213-5](https://doi.org/10.1016/S0022-4596(03)00213-5).
- [27] H.J. Monkhorst, and J.D. Pack, Physical Review B, **13**, 5188 (1976), <https://doi.org/10.1103/PhysRevB.13.5188>.
- [28] A. Khan, M. Sajjad, G. Murtaza, and A. Laref, Zeitschrift für Naturforschung A, **73**, 645-655 (2018), <https://doi.org/10.1515/zna-2018-0070>.
- [29] L. Isaenko, A. Yelisseyev, S. Lobanov, P. Krinitsin, V. Petrov, and J.J. Zondy, J. Non-Crystalline Solids, **352**, 2439-2443 (2006), <https://doi.org/10.1016/j.jnoncrysol.2006.03.045>.
- [30] R. Khenata, A. Bouhemadou, M. Sahnoun, A.H. Reshak, H. Baltache, and M. Rabah, Computational Materials Science, **38**, 29-38 (2006), <https://doi.org/10.1016/j.commatsci.2006.01.013>.
- [31] J. Sun, H.T. Wang, N.B. Ming, Applied Physics Letters, **84**, 4544-4546 (2004), <https://doi.org/10.1063/1.1758781>.
- [32] B. Mayer, H. Anton, E. Bott, M. Methfessel, J. Sticht, J. Harris, and P. C. Schmidt, Intermetallics, **11**, 23-32 (2003), [https://doi.org/10.1016/S0966-9795\(02\)00127-9](https://doi.org/10.1016/S0966-9795(02)00127-9).
- [33] H. Fu, D. Li, F. Peng, T. Gao, and X. Cheng, Computational Materials Science, **44**, 774-778 (2008), <https://doi.org/10.1016/j.commatsci.2008.05.026>.
- [34] D.G. Pettifor, Materials Science and Technology, **8**, 345-349 (1992), <https://doi.org/10.1179/mst.1992.8.4.345>.
- [35] S.F. Pugh, Philosophical Magazine and J. Science, **45**, 823-843 (1954), <https://doi.org/10.1080/14786440808520496>.
- [36] R. Hill, Proceedings of the Physical Society. Section A, **65**, 349 (1952), <https://doi.org/10.1088/0370-1298/65/5/307>.
- [37] T. Lantri, S. Bentata, B. Bouadjemi, W. Benstaali, B. Bouhafs, A. Abbad, and A. Zitouni, J. Magnetism and Magnetic Materials **419**, 74-83 (2016), <https://doi.org/10.1016/j.jmmm.2016.06.012>.
- [38] S. Sharma, A.S. Verma, and V.K. Jindal, Materials Research Bulletin, **53**, 218-233 (2014), <https://doi.org/10.1016/j.materresbull.2014.02.021>.
- [39] C.M.I. Okoye, J. Physics: Condensed Matter, **15**, 5945-5958 (2003), <https://doi.org/10.1088/0953-8984/15/35/304>.

ОСНОВНІ ФІЗИЧНІ ВЛАСТИВОСТІ СТРУКТУРОВАНИХ СПОЛУК ХАЛЬКОПІРИТУ LiInS_2 та LiInSe_2

Джуоті Кумар^a, Шаліні Томар^a, Сухендра^b, Банварі Лал Чоудхарі^a, Упасана Рані^a, Аджай Сінх Верма^c

^aФізичний факультет, Банастанлі Від'яніт, Раджастан, (Індія) 304022

^bФізичний факультет, Меморіальний коледж GDC, Бахал, Бхівані, (Індія) 127028

^cФакультет природничих та прикладних наук, Університет Глокал, Сахаранпур (Індія) 247232

Для деяких сполук халькопіриту ми теоретично вивчили їхні різні властивості, наприклад структурні, електронні, оптичні та механічні. Криву зонної структури, щільність станів, а також загальну енергію досліджували за допомогою ATK-DFT методом псевдопотенціальної плоскої хвилі. Для халькопіритів LiInS_2 та LiInSe_2 ми виявили, що ці сполуки мають пряму енергетичну щільну, яка становить 3,85 eV та 2,61 eV для LiInS_2 та LiInSe_2 , відповідно. Це показує, що ширина енергетичної щільності зменшується від «S» до «Se», а також відношення V/G , яке називається коефіцієнтом П'ю, становить 2,10 для LiInS_2 та 2,61 для LiInSe_2 , таким чином ці сполуки є пластичними за своєю природою, також ці сполуки виявляються механічно стабільними. Дослідження цієї роботи показує, що пара цих сполук халькопіриту може бути перспективним кандидатом для заміни поглинаючого шару у фотоелектричних пристроях.

Ключові слова: неемперічні (Ab-initio) розрахунки; електронні властивості; оптичні властивості; пружні константи